Dimensionless ratios: characteristics of quantum liquids and their phase transitions

Yi-Cong Yu,[1] Yang-Yang Chen,[1] Hai-Qing Lin,[2, *] Rudolf A. Römer,[3] and Xi-Wen Guan[1, 4, 5, †]

[1]State Key Laboratory of Magnetic Resonance and Atomic and Molecular Physics,
Wuhan Institute of Physics and Mathematics, Chinese Academy of Sciences, Wuhan 430071, China
[2]Beijing Computational Science Research Center, Beijing 100094, China
[3]Department of Physics and Centre for Scientific Computing,
University of Warwick,a Coventry, CV4 7AL, UK
[4]Center for Cold Atom Physics, Chinese Academy of Sciences, Wuhan 430071, China
[5]Department of Theoretical Physics, Research School of Physics and Engineering,
Australian National University, Canberra ACT 0200, Australia
(Dated: *Revision* : 1.2, compiled November 24, 2016)

Dimensionless ratios of physical properties can characterize low-temperature phases in a wide variety of materials. As such, the Wilson ratio (WR), the Kadowaki-Woods ratio and the Wiedemann-Franz law capture essential features of Fermi liquids in metals, heavy fermions, etc. Here we prove that the phases of many-body interacting multi-component quantum liquids in one dimension (1D) can be described by WRs based on the compressibility, susceptibility and specific heat associated with each component. These WRs arise due to additivity rules within subsystems reminiscent of the rules for multi-resistor networks in series and parallel — a novel and useful characteristic of multi-component Tomonaga-Luttinger liquids (TLL) independent of microscopic details of the systems. Using experimentally realized multi-species cold atomic gases as examples, we prove that the Wilson ratios uniquely identify phases of TLL, while providing universal scaling relations at the boundaries between phases. Their values within a phase are solely determined by the stiffnesses and sound velocities of subsystems and identify the internal degrees of freedom of said phase such as its spin-degeneracy. This finding can be directly applied to a wide range of 1D many-body systems and reveals deep physical insights into recent experimental measurements of the universal thermodynamics in ultracold atoms and spins.

I. INTRODUCTION

One of the central challenges in condensed matter physics is to understand how different phases of matter can arise and how these phases can be characterized. Many phenomena such as, e.g., superconductivity, magnetism and quantum phase transitions in strongly correlated systems [1], Bose-Einstein condensation of dilute gases [2] and of excitons in semiconductors, electronic transport in low-dimensional systems and heavy-fermion physics [3], are known to exist due to the *collective* nature of the underlying many-body processes. Collective phenomena are particularly strong in low-dimensional systems where the reduced dimensionality enhances the interaction of elementary constituents [4–7]. In order to characterize the various phases, dimensionless ratios such as the celebrated Wiedemann-Franz (WF) law [8] or the Kadowaki-Wood ratio [9, 10] are very useful. They usually involve ratios of measurable quantities which stem from similar underlying processes.

The WF law is universal across a wide range of materials and temperature regimes because non-universal contributions due to, e.g., density of states and effective mass often cancel out. Conversely, deviations from the WF law can be used to characterize the emergence of new physical processes [11]. Remarkably, recent new

experiments [12] show that the WF law holds even at quantum phase transitions. Similarly, the Wilson ratio (WR) [13, 14],

$$R_{\mathrm{W}}^{\chi} = \frac{4}{3}\left(\frac{\pi k_B}{\mu_B g_{\mathrm{Lande}}}\right)^2 \frac{\chi}{c_V/T}, \qquad (1)$$

between the susceptibility χ and the specific heat c_V divided by the temperature T, measures the strength in magnetic fluctuations versus thermal fluctuations [3, 15, 16]. Here k_B is Boltzmann's constant, μ_B is the Bohr magneton and g_{Lande} is the Lande factor. This dimensionless ratio has been observed in a wide variety of Kondo systems [3, 14]. Recent studies of the WR for magnetic states of a 1D spin ladder compound [17] and the two-component attractive Fermi gas [18] show that R_{W}^{χ} allows a convenient identification of magnetic phases. Dimensionless ratios therefore provide an elegant experimental and theoretical approach to a qualitative and quantitative characterization of the nature of complex multi-component quantum liquids.

In Fig. 1, we show that the *Wilson-like* ratio

$$R_{\mathrm{W}}^{\kappa} = \frac{\pi^2 k_B^2}{3}\frac{\kappa}{c_V/T}, \qquad (2)$$

relating particle fluctuations to energy fluctuations, is even more successful in determining phases in quantum liquids. Recent experiment [19] show that the compressibility WR (2) determines the Luttinger parameter for the phase of TLL in 1D Bose gases and characterizes the quantum fluctuations at quantum criticality. The key ob-
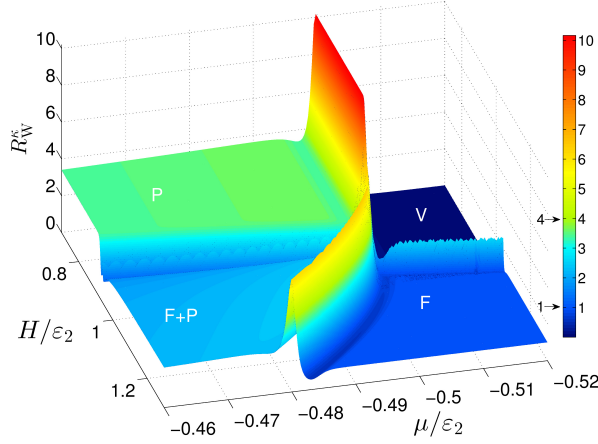
FIG. 1: Phase diagram for the attractive SU(2) Yang-Gaudin model at $T = 0.001\varepsilon_2/k_B$ given as 3D plot of the WR R_W^κ in the $\mu - H$ plane. The pair binding energy is denoted by $\varepsilon_2 = 0.5$ and the interaction strength $g_{1D} = -2$. The expected values of $R_W^\kappa = 1, 4$ in the excess fermion phase (F) and the pure pair phase (P) in strong coupling limit, respectively, are indicated on the legend on the right. The mixed phase of fermions and pairs is denoted as F+P.

servation underlying the predictive strength of both WRs is that the phases are related to simple *additivity rules* of the underlying elementary excitations. In this paper, we shall prove that such additivity rules are in fact general for multi-component quantum liquids in 1D — and we expect that they also hold for multicomponent Fermi liquids in higher dimensions [16]. We further show that both WRs stem from these exact additivity rules, can quantitatively identify quantum phases of Tomonaga-Luttinger liquids (TLL) independent of microscopic details and exhibit universal scaling behavior at the quantum transitions between phases. Their values within a given phase give information about the internal degrees of freedom of a phase, e.g., its spin-degeneracy. Such information is important, e.g., for the collective nature of multicomponent interacting quantum liquids in cold atoms [20–23], large-symmetry fermionic systems [24, 25], spin chains [17, 26] and 1D Hubbard model [5].

II. THEORY

A. General considerations

In order to show the versatility of the WRs in identifying phases, we are interested in systems that have a rich phase diagram. We therefore start by studying first an attractive quantum liquid that supports a hierarchy of bound states. The system shall consist of unbound particles, pairs of particles, triples of particles and so on until we have at most w-tuples. For convenience, we shall denote a bound state formed from r particles as

a *r-complex*. Let N_r denote the number of r-complexes which have formed. Then the total number of particles is given as $N = N_1 + \ldots + wN_w$ and the density of a r-complex is $n_r = N_r/L$ such that the total particle density is $n = \sum_{r=1}^{w} rn_r$. The relative propensity of a phase is governed by a set of external fields H_r, $r = 1, \ldots, w$ with $H_w = 0$. Here the H_r are coupling to the (spin) moment of each r-complex. Then we can write for the Hamiltonian of the system

$$\mathcal{H} = \mathcal{T} + \mathcal{V} - \sum_{r=1}^{w-1} H_r N_r - \mu N, \qquad (3)$$

where $\mathcal{T}$ and $\mathcal{V}$ are as of yet unspecified kinetic and many-body interaction energies.

In order to compute the WRs (1) and (2), we need to compute the susceptibility χ, the compressibility κ and specific heat c_V for the w-component system in the Gibbs ensemble $G(\mu, H_1, \ldots, H_w)$. In a single compnent system, χ and κ can be straightforwardly computed as $\partial M/\partial H$ (with magnetization M) for constant particle number (canonical) or $\partial n/\partial \mu$ for constant external fields (grand canonical). For a multi-component system, we therefore define in complete analogy a chemical potential μ_r for each of the r-complexes via

$$\mu_r = \mu + \frac{1}{r}H_r + \frac{\varepsilon_r}{r}, \qquad (4)$$

where ε_r denotes the binding energy of an r-complex. Remarkably, the quantity μ_2 has already been measured in a recent experimental study of the equation of state for 2D ultracold fermions [23]. It gives a deep physical insight into the crossover from Bose-Einstein condensate to Bardeen-Cooper-Schrieffer superconductor. Indeed, the choice (4) allows us to define a Fermi energy at $T = 0$ for each fluid of r-complexes in the same way that ϵ_F is defined in the Landau's Fermi liquid picture. We now introduce a *stiffness* in grand canonical and canonical ensembles, respectively, as

$$D_r^\kappa = \frac{r}{\hbar\pi}\left(\frac{\partial\mu_r}{\partial n_r}\right)_{H_1,\ldots,H_{w-1}}, \quad D_{r,r'}^\chi = \frac{r}{\hbar\pi}\left(\frac{\partial\mu_r}{\partial n_{r'}}\right)_n (5)$$

for a r-complex fluid subject to μ and the field $H_{r'}$. Also, the *sound velocity* for r-complexes is defined as usual via $v_r = \frac{d\epsilon_r(k)}{dk}|_{k_F}$, where $\epsilon_r(k)$ is the dispersion relation for r-complexes and k_F the Fermi momentum. With these definitions, we can then prove in 1D that the individual κ_r, χ_r and $c_{V,r}$ in terms of the D_r^κ, $D_{r,r'}^\chi$ and v_r are given as

$$\kappa_r = \frac{r^2}{\pi\hbar}\frac{1}{D_r^\kappa}, \quad \chi_{r,r'} = \frac{r^2}{\pi\hbar}\frac{1}{D_{r,r'}^\chi}, \quad c_{V,r} = \frac{\pi k_B^2 T}{3\hbar}\frac{1}{v_r} (6)$$

as shown in the Appendix. We note that similar relations hold in Fermi liquids (FLs) [16]. Our strategy therefore is to derive the densities n_r, the chemical potentials μ_r and the dispersions $\epsilon_r(k)$ for the r-complexes as functions

of $H_1, \ldots, H_w$ and μ. We expect that the definitions (5) and (6) are useful in general for interacting quantum liquids. However, analytical or numerical access to these quantities is not necessarily straightforward. Following a series of recent papers [27], we prove here that integrable 1D multi-component systems allow the explicit construction of n_r, μ_r and ϵ_r using the thermodynamic Bethe Ansatz (TBA) [28–30]. Following earlier theoretical [16] and recent experimental [19, 23] findings, we furthermore speculate that similar relations also hold for FLs in higher dimensions and expect that such effective chemical potentials for multi-component systems can therefore serve as convenient handles to describe multi-component quantum liquids.

B. The w-component quantum liquid

Let us now consider a specific w-component Hamiltonian (3) that supports multi-component quantum liquids. A convenient and experimentally relevant example is the 1D SU(w) Fermi gas with δ-function interaction confined to length L [31, 32]. The system is described by the Hamiltonian (3) with

$$\mathcal{T} + \mathcal{V} = -\frac{\hbar^2}{2m} \sum_{i=1}^{N} \frac{\partial^2}{\partial x_i^2} + g_{1D} \sum_{1 \le i < j \le N} \delta(x_i - x_j), \quad (7)$$

and with the chemical potential μ and the effective Zeeman energy $E_z = \sum_{r=1}^{w} \frac{1}{2} r(w-r) n_r H_r$. There are w possible hyperfine states $|1\rangle, |2\rangle, \ldots, |w\rangle$ that the fermions can occupy. Experimentally, g_{1D} ($= -2\hbar^2/ma_{1D}$, with a_{1D} the effective scattering length in 1D [33]; from now on, we choose our units such that $\hbar^2 = 2m = 1$ unless we particularly use the units.) can be tuned from a weak interaction to a strong coupling regime via Feshbach resonances. This model provides an ideal experimental testing ground to probe few- and many-body physics [34, 37, 38].

For the system described by (7), the relation (4) follows naturally from the structure of the TBA equations [27] (see Appendix A). We will use in addition general energy-transfer relations for breaking a w-complex into smaller r-complexes, i.e.

$$\frac{1}{r} H_r = \mu_r - \mu_w + \frac{1}{w} \varepsilon_w - \frac{1}{r} \varepsilon_r \quad (8)$$

with $r = 1, 2, \ldots, w - 1$. Note that $\varepsilon_r = \frac{1}{48} r (r^2 - 1) g_{1D}^2$ is the explicit binding energy for each r-complex in the system (7). Using the energy and particle conservation conditions, (8) and $n = \sum_{r=1}^{w} r n_r$, respectively, we find that κ and χ_r obey the additivity rules,

$$\kappa = \kappa_1 + \kappa_2 + \cdots + \kappa_w, \quad (9)$$

$$\frac{1}{\chi_r} = \frac{1}{\chi_{r,1}} + \frac{1}{\chi_{r,2}} + \cdots + \frac{1}{\chi_{r,w}}. \quad (10)$$

in the TLL phases (see Appendix B). Here the susceptibility χ_r represents the responses of different bound

states to the change of the field H_r. Such additivity appears naturally for a non-interacting fluid. Determining v_r from the TBA, we similarly find that

$$c_V = c_{V,1} + c_{V,2} + \cdots + c_{V,w}. \quad (11)$$

Based on the rules given in (9), (10) and (11), we can construct the WRs of the w-component SU(w) system to be

$$R_{W,r'}^\chi = \left(\sum_{r=1}^{w} \frac{D_{r,r'}^\chi}{r^2} \right)^{-1} \left(\sum_{r=1}^{w} \frac{1}{v_r} \right)^{-1}, \quad (12)$$

$$R_W^\kappa = \left(\sum_{r=1}^{w} \frac{r^2}{D_r^\kappa} \right) \left(\sum_{r=1}^{w} \frac{1}{v_r} \right)^{-1}. \quad (13)$$

These ratios are dimensionless and uniquely determined by the sound velocities and stiffnesses. We note that the form of the WRs in (12) and (13) is similar for a w-component FL; all interaction effects have been included into (8) via the choice of μ_r.

In the strong coupling regime, R_W^κ for a pure r-complex phase ($R_W^\chi = 0$ in pure phases [18]) can be given in the form

$$R_W^{\kappa,r} = rK_r = r^2 \left(1 - 2B_r \frac{1}{|\gamma|} + B_r^2 \frac{1}{\gamma^2} \right) + O(\gamma^{-3}), (14)$$

where $\gamma = g_{1D}/2n$ is the dimensionless interaction strength, $B_1 = 0$ and $B_r = \sum_{k=1}^{r-1} 1/k$ with $r = 2, \ldots, w$. In the above equation, K_r is the phenomenological Luttinger parameter which can be directly measured through the Wilson ratio R_W^χ. This provides an important way to test the low energy Luttinger theory. For $\gamma \to \infty$, R_W^κ then displays plateaus at the integers $1^2, \ldots, r^2, \ldots, w^2$. Deviations from integer $r^2 = 1, 4, 9$, occur not because of a weakness of the ratios introduced here, but because of the physics underlying and determining the stability and mixture of bound states in a given phase. Thus R_W^κ provides a convenient *quantitative* phase characteristic for quantum systems at finite T as well as at $T = 0$, see Fig. 1 and below.

C. Scaling of the WRs

It is particularly interesting that the WRs identify non-TLL behaviour and quantum criticality in the quantum critical regime. In fact, the WRs show sudden enhancement near a quantum phase transition due to a breakdown of the quantum liquid nature, i.e. the vanishing linear dispersion for 1D systems. For both WRs, we have the scaling law

$$R_W^{\kappa,\chi} = \mathcal{F}^{\kappa,\chi} \left[\frac{(\eta - \eta_c)}{T^{\frac{1}{\nu z}}} \right] + \lambda_0 T^{-\beta} \mathcal{G}^{\kappa,\chi} \left[\frac{(\eta - \eta_c)}{T^{\frac{1}{\nu z}}} \right], (15)$$

where $\beta = (d/z) + 1 - 2/(\nu z)$ with $z = 2$, $\nu = 1/2$ and $d = 1$ for 1D systems is universal; $\mathcal{F}^{\kappa,\chi}$, $\mathcal{G}^{\kappa,\chi}$ are
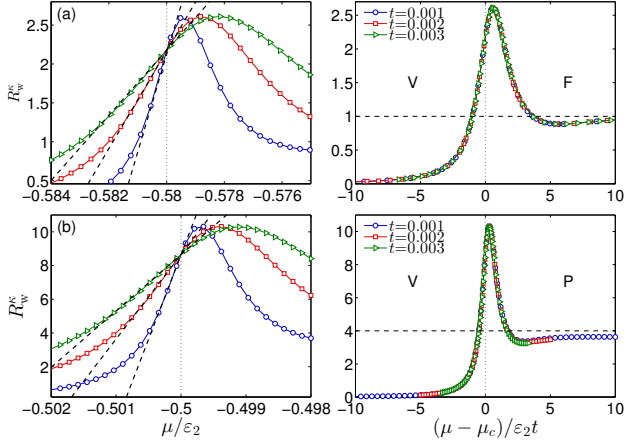
FIG. 2: Scaling of R_W^κ at phase boundaries (a) V-F and (b) V-P with $H/\epsilon_2 = 1.16$ and 0.9, respectively (cp. Fig. 1). The left panels in (a) and (b) show R_W^κ vs. μ/ϵ_2 for reduced temperatures $t = 0.003$ ($\triangle$), 0.002 ($\square$) and 0.001 ($\circ$). The vertical dotted lines indicate μ_c/ϵ_2. The dashed lines show the calculated slopes C_r/t. The right panels show the scaled R_W^κ as in (15) with $\beta = -1/2$ vs. $(\mu - \mu_c)/\epsilon_2 t$. The vertical dotted lines are as in the left panel while the horizontal lines indicate the strong interaction limit of R_W^κ in the (a) F and (b) P phases.

the scaling functions (see Appendix C). The second term in (15) with $\beta = -1/2$ reflects a contribution from the background at the temperatures above the energy gap $\Delta \sim |\eta - \eta_c|^{zv}$, with driving parameter η (e.g. μ or H_r). These critical exponents agree with the experimental result for the thermal and magnetic properties of the 1D spin chain at criticality [19, 26]. For a phase transition from the vacuum to a TLL phase, $\lambda_0 = 0$. Based on (15), the slope of the temperature-rescaled R_W^κ curves at a critical point is given by $\left(\frac{\partial R_W^\kappa}{\partial \mu}\right)_{\mu_c} = C_r/T$, see Appendix C.

The significance of the WRs can also be understood from the quantum fluctuations of magnetization, $\langle \delta M^2 \rangle = \ell^d k_B T \chi$, and particle number, $\langle \delta N^2 \rangle = \ell^d k_B T \kappa$; ℓ^d denotes the observation volume in d-dimensions. Therefore, microscopically, χ and κ measure the strength of these fluctuations just as c_V quantifies the energy fluctuations; macroscopically, the temperature-independent compressibility and the linear-temperature-dependent specific heat remarkably preserve the nature of quantum liquid at the renormalization fixed point, see Eq. (6) like the Fermi liquid [15]. Consequently, R_W^χ and R_W^κ characterise the competition between fluctuations of different origin. A constant WR implies that the two types of fluctuations are on an equal footing, regardless of the microscopic details of the underlying many-body system. On the other hand, the growth of the WRs in the critical regime indicates the long-range character of the quantum fluctuations at the quantum phase transitions.

III. APPLICATIONS

A. The Yang-Gaudin model.

In order to show the usefulness of the new ratios, we start by considering the $w = 2$ 1D spin-1/2 Fermi gas with a δ-function interaction [35, 36]. This Yang-Gaudin model has already provided an ideal experimental testing ground [34, 37, 38] for few- and many-body physics [27, 39, 40]. For R_W^χ, the additivity rule of susceptibility and its connection to the D_r^χ's following (12) have been reported in [18]. For R_W^κ, we now find from (13) that

$$R_W^\kappa = \left(\frac{1}{D_1^\kappa} + \frac{4}{D_2^\kappa}\right) / \left(\frac{1}{v_1} + \frac{1}{v_2}\right). \quad (16)$$

Writing the explicit dependence on μ, H and g_{1D} is possible, but tedious (we give explicit forms for $D_{1,2}^\kappa$ and $v_{1,2}$ in Appendix B). In Fig. 1 we show R_W^κ in the μ–H plane. R_W^κ elegantly maps out the three finite temperature TLL phases of 1-complexes, i.e. fully-polarized fermions (F), 2-complexes, i.e. pairs (P), and the mixed TLL of excess fermions and pairs (F+P). The empty vacuum phase (V) is also present in Fig. 1. In particular, we note that for the pure phases F and P, $R_W^\kappa \approx r^2$, i.e. close to the strong coupling value rK_r [41]. Hence for the Yang-Gaudin model in Fig. 1 we see $R_W^\kappa = 1$ in phase F and 4 in phase P. In mixed phases, e.g. F+P, such a constant plateau no longer exists. For R_W^κ in the critical regime, we find a rapid increase due to a strong increase in thermal fluctuations. In Fig. 2 we show the scaling behavior (15) for R_W^κ close to the transition from the vacuum phase into the F and the P phases. We find $C_1 \approx 1.2546$ and $C_2 \approx 2 \times 5.0185$, respectively. Eq. (15) does not contain any free fitting parameter, so one can use this scaling to determine the temperature of the quantum liquid. The scaling law is also similar to the scaling in the non-FL regime of heavy fermions [3, 42].

B. A $w \geq 3$ quantum liquid.

An even richer phase diagram exists for the three-component δ-function interacting Fermi gas with an attractive interaction [31]. Its $T = 0$ phases are known to consist of excess fermions (F), pairs (P), trions (T) and mixtures thereof [43, 44]. Using the TBA equations, we again numerically and analytically calculate the WRs and determine their H_1, H_2 and T dependencies. In Fig. 3 we show that in the pure phases F, P and T, we have $R_W^\kappa = 1, 4, 9$, respectively, and the phase boundaries are clearly marked by large increases in R_W^κ near the critical points. At $T > 0$, we see that the κ and c_V curves become progressively more rounded across the phase transitions for T increases. The magnetic field associated with the position of the finite-height peaks varies as a function of temperature. This can be used to define a crossover temperature T^* for each such magnetic field
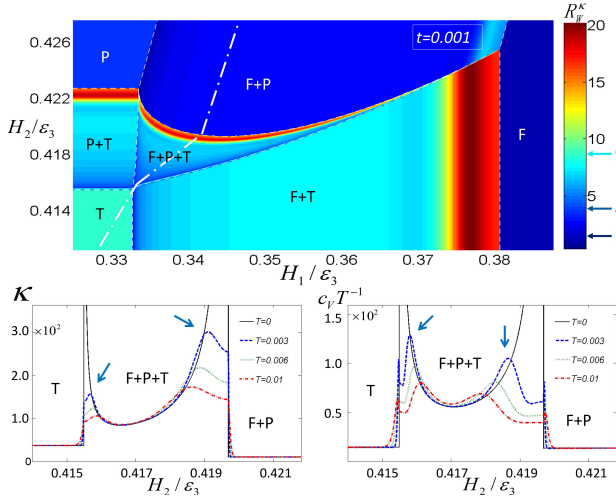
FIG. 3: Upper panel: plot of R_W^κ for the 1D three-component attractive Fermi gas in the H_1–H_2 plane at temperature $t = 0.001\varepsilon_3/k_B$. The values of $R_W^\kappa = 1, 4, 9$ in the pure phases F, P and T, respectively, are indicated by the colors marked on the color scale shown. The dashed lines follow the phase boundaries as indicated. Lower panel: compressibility κ and specific heat c_V/T vs. external field H_2/ε_3 for a fixed choice of polarization $n_1 = n_2$ indicated by the dash-dotted line in the phase diagram (upper panel). At zero temperature, κ and c_V/T satisfy the additivity rules (9) and (11) as shown by the solid lines while at finite T, they exhibit peaks as indicated by the arrows for $t = 0.003\varepsilon_3/k_B$. Near the phase boundaries both κ and c_V/T diverge quickly as $(H_2 - H_2^c)^{-1/2}$.

corresponding to a peak. For $T < T^*$, our analytical and numerical results reconfirm the validity of the additivity rules (9)–(11), i.e. κ and χ remain independent of the temperature and c_V depends linearly on the temperature in the TLL phase (cp. lower panel in Fig. 3). This nature is also seen in Fermi liquids [14, 15]. The additivity nature of the susceptibility is presented in Appendix B. The significance of such additivity rules is the characteristic of quantum liquids at the renormalization fixed point, such as TLLs in integrable models and Fermi liquids in metals. etc. For $T > T^*$, R_W^κ exhibits the critical scaling behaviour (15) (see also Appendix C). Fig. 4 shows the contour plot of R_W^κ at low temperatures. The universal quantum critical behaviour (15) is characterized by the exponents $z = 2, \nu = 1/2$. For $T < T^*$, the critical exponents are $z = \nu = 1$.

Moreover, using the TBA equations for the $SU(w)$ Fermi gases with an attractive interaction [45], we calculate the susceptibility $\chi_r = \partial M/\partial H_r$ in response to the change of magnetic field H_r for the *spin-gapped* phases. The other magnetic fields are fixed and the magnetization is given by $M = \sum_{r=1}^{w-1} n_r r(w-r)/2$. In dimensionless units, the energies are rescaled by the interaction energy $\epsilon_b = \frac{1}{2}\hbar^2 c^2/(2m)$, i.e. the temperature $t = T/\epsilon_b$, the pressures $\tilde{p}^r = p^r/(|c|\epsilon_b)$, the susceptibility $\tilde{\chi} = |c|\xi/2$, see the Appendix B. We obtain explicitly a general expression of the susceptibility χ_r for the gapped phase in which a small number of the $r-$complexes are created
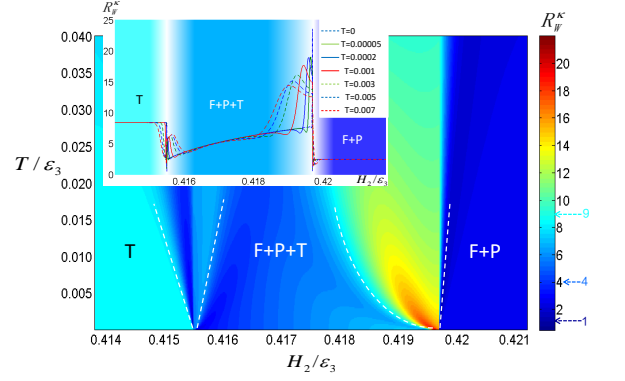
due to the change of H_r for $t \ll 1$,

$$\tilde{\chi}_r \approx \frac{1}{4\sqrt{2\pi}} \frac{1}{\sqrt{t}} \sqrt{r}(w-r)re^{-\frac{\Delta_r}{t}}, \qquad (17)$$

where the gap is given by

$$\Delta_r \approx -r\tilde{\mu}_r + \sum_{m=1}^{w} \sum_{\substack{q = 1 \\ 2q \neq r + m}}^{\min(r,m)} \frac{4\tilde{p}^m}{m(r+m-2q)}, \qquad (18)$$

see the Appendix C. For example, from the upper panel phase diagram in Fig. 3, we observe that in the gapped phase of T, $\tilde{\chi}_1$ with $\Delta_1 = -\tilde{\mu}_1 + 2\tilde{p}^3/3$ and $\tilde{\chi}_2$ with $\Delta_2 = -2\tilde{\mu}_2 + 16\tilde{p}^3/9$ show a dilute magnon behaviour related to the phase transitions from the phase T into the mixed phase F+T and into the the mixed P+T, respectively. They decay exponentially as the temperature approaches zero. By properly choosing H_1 and H_2, we also can have a phase transition from the gapped phase T into the mixed phase F+P+T.

C. Critical theory for the $SU(w)$ repulsive Fermi gases

The existence of internal degrees of freedom significantly changes the quantum magnetism and the dynamics of the system compared to the spinless Bose gas. It is well established that the critical behaviour of the spin $SU(w)$ chain can be described by the Wess-Zumino-Witten σ model of level $\ell = 1$ with the Kac-Moody central charge $C_s = \ell(w^2-1)/(\ell+w)$ [49]. The w-component repulsive Fermi gases display a $U(1) \otimes SU(w)$ symmetry characterized by one charge degree of freedom and $w - 1$

FIG. 4: Mapping out quantum criticality with R_W^κ in the T–H_2 plane. The H_2 values have been chosen to follow the fixed polarization $n_1 = n_2$ as indicated by the dash-dotted white line in Fig. 3. The white dashed lines denote the crossover temperatures T^* beyond which the TLL phases break down. The inset shows individual temperature curves of R_W^κ vs. H_2 for representative temperatures. The bold solid line shows the result corresponding to (13) while the thin dashed lines show the numerical results obtained from the TBA equations (Appendix A).

spin rapidities. The low-energy physics of the system is described by the spin-charge separated conformal field theories of an effective Tomonaga-Luttinger liquid and an antiferromagnetic $SU(w)$ Heisenberg spin chain [5, 50]. By using the TBA equations given in [45] with $H \to 0$ we find that the pressure of the 1D repulsive Fermi gases is given by

$$p = p_{T=0} + \frac{w(w^2-1)H^2}{24\pi v_s} + \frac{\pi T^2}{6}\left[\frac{1}{v_c} + \frac{C_s}{v_s}\right], \quad (19)$$

where $p_{T=0}$ is the pressure at $T = 0$ and $v_{s,c}$ are the pseudo Fermi velocities in the spin and charge sectors, respectively. This result is consistent with the critical field theory for the $SU(w)$ spin chains [49]. In the zero magnetic field limit, the spin and charge velocities for the Fermi gas with strong repulsion are, respectively,

$$v_s = \frac{2n^2\pi^3 a_{1D}}{3w}(1 + 3a_{1D}Z\,n),$$
$$v_c = 2n\pi(1 + 2a_{1D}Z\,n), \quad (20)$$

where $Z = -\frac{1}{w}\left[\psi(\frac{1}{w}) + C\right]$ and C the Euler γ-constant, $\psi(x)$ the Euler ψ-function. The susceptibility is then given by Luttinger-liquid relation

$$\chi v_s = \frac{1}{12\pi}w(w^2-1) \quad (21)$$

in the limit $H \to 0$. Indeed the sound velocity v_c (20) of the Fermi gas in the large-w limit coincides with that for the spinless Bose gas, whereas v_s vanishes quickly as w grows. This gives a reason why the quantum liquid of multi-component fermions reduces to the liquid of a spinless Bose gas in this limit [34]. In this sense, R_W^χ captures this unique large-spin charge separation mechanism in the w-component repulsive Fermi gas. Its explicit expressions is

$$R_W^\chi = \frac{w(w^2-1)v_c}{3\left[(w-1)v_c + v_s\right]}, \quad (22)$$

displaying plateaus of height $w(w+1)/3$ for either strong repulsion or in the large-w limit, hence capturing the spin degeneracy. For example, $R_W^\chi = 2$ and 4 for the two- and three-component Fermi gases with strong repulsion, respectively.

IV. EXPERIMENTAL REALIZATIONS

Both WRs R_W^χ and R_W^κ are readily accessible by experiments. For example, the 1D $SU(w)$ δ-function interacting Fermi gas of ^{173}Yb has been realized experimentally [34]. It was shown that in the large-w limit the ground state of the gas with a repulsive interaction exhibits properties of a bosonic spinless liquid. In the context of ultracold atoms, it is highly desirable to measure the quantum criticality and the TLL in such
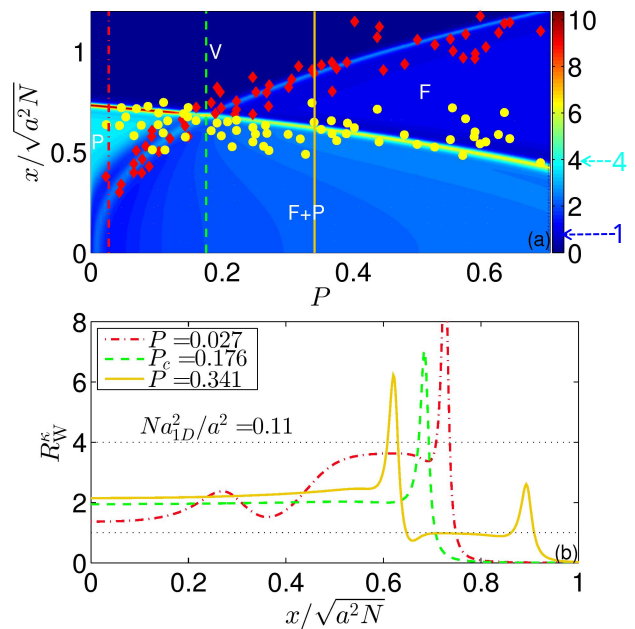

FIG. 5: Upper panel: Contour plot of the WR R_W^κ (2) for the Yang-Gaudin model in a harmonic trap with fixed particle number N and three different polarizations $P = n_1/n$ at the temperature $T = 0.001\varepsilon_2/k_B$. The WR evolves thin round peaks near the phase boundaries, whereas the values of the WR (16) quantify different quantum phases of the TLLs. The WR peaks are in good agreement with the experimental phase boundaries (red and yellow dots) observed in [37]. Lower panel: the red-dashed and yellow-solid lines show the WR R_W^κ in the trapped gas with the polarizations $P = 0.027$ and $P = 0.341$, respectively. They indicate segments of the Fulde-Ferrell-Larkin-Ovchinnikov (FFLO) phase in the centre accompanied by the wings of the P and the F states, respectively. The highest R_W^κ plateau approaches 4 suggesting a quasi-1D superfluid nature, whereas the lowest plateau shows the free fermion nature with $R_W^\kappa = 1$. For a critical polarization $P_c = 0.176$, the green-dashed line shows that the trapped gas consists solely of the FFLO-like state.

Fermi gases with rich spin and charge degrees of freedom. In this scenario, the Yang-Gaudin model is an ideal model to conceive critical phenomena induced from spin and charge interaction effects. This model was recently studied via an ultracold atomic gas in a harmonic trap, such as the two-component ultracold ^{6}Li atoms of Ref. [37]. Due to the harmonic confinement, the chemical potential in the equation of state should be replaced by $\mu(x) = \mu(0) - m\omega^2 x^2/2$ (within the local density approximation). Here x denotes the position along the 1D trap. Changing x is then equivalent to changing μ and different phases are located at different spatial positions along the trap. Using a rescaled coordinate $y = xa_{1D}/(2a^2)$ with axial characteristic oscillation length $a = \sqrt{\hbar/m\omega}$, the density profile of the trapped gas can be determined from the dimensionless quantities $Na_{1D}^2/a^2 = 2a_{1D}\int_{-\infty}^{\infty} dy\, n(y)$ and polarization

$Ma_{1D}^2/a^2 = 2a_{1D}\int_{-\infty}^{\infty} dy\, m_z(y)$. The compressibility can be extracted via $\kappa = \partial n/\partial \mu = -\partial n/\partial x/(xm\omega^2)$ [46, 47], while the density $n(x)$ is read off from experimental profiles along x. The specific heat can be measured through the sound velocities, while the density waves of pairs and unpaired fermions can be experimentally created by a density depletion or pulse with a far-detuned laser beam [48]. In the upper panel of the Fig. 5, we observe that R_W^κ at a very low temperature naturally maps out the phase diagram of the system, showing a good agreement with the experimental phase boundaries [37]. In the lower panel of Fig. 5, we show the behaviour for R_W^κ, exhibiting the plateau structure as the system passes through different phases upon changing x.

V. CONCLUSIONS

In summary, we have shown that the additivity rules of physical properties reveal an important characteristic of the TLL and provide the physical origin of the dimensionless WRs. Such dimensionless ratios can be used to identify full TLL phases and capture the essence of phenomena ranging from quantum criticality to spin and charge separation in a wide variety of 1D many-body systems. We have presented some universal relations, such as the WRs (12) and (13), the Luttinger parameter (14), the dimensionless scaling function of the WR (15), the susceptibility for the gapped systems (17) and the WR of $SU(w)$ repulsive Fermi gas related to the level-1 Wess-Zumino-Novikov-Witten conformal theory (22). We also show excellent agreement between the phase diagram predicted by the WRs and the experimentally determined one for

the Yang-Gaudin model [37]. Our results therefore successfully demonstrate how to predict universal laws for experimentally realizable quantum liquids in Bose and Fermi degenerate gases, Bose-Fermi mixtures, 1D Hubbard model, strongly correlated electronic systems, spin compounds near to and far from quantum critical points on an equal footing.

Appendix A: Thermodynamic Bethe Ansatz for the SU(w) Fermi gas

The Gibbs free energy of the $SU(w)$ attractive gas is

$$G(\mu, H_1, \ldots, H_w) = \sum_{r=1}^{w} \frac{rT}{2\pi} \int dk \ln\left[1 + e^{-\epsilon_r(k)/T}\right] \tag{A1}$$

with dispersions $\epsilon_r(k)$ defined in the TBA via

$$
\begin{aligned}
\epsilon_r(k) =\ & rk^2 - r\mu - H_r - \varepsilon_r + \sum_{p=1}^{r-1}\left\{ \sum_{q=p}^{w} a_{q+r-2p} * T\ln\left[1 + e^{-\epsilon_q(k)/T}\right] + \sum_{q=r+1}^{w} a_{q-r} * T\ln\left[1 + e^{-\epsilon_q(k)/T}\right] \right\} \\
& - \sum_{q=1}^{\infty} a_q * T\ln\left[1 + e^{-\eta_{r,q}/T}\right],
\end{aligned}
\tag{A2}
$$

$$
\begin{aligned}
\eta_{r,l}(k) =\ & l\cdot(2H_r - H_{r-1} - H_{r+1}) + a_l * T\ln\left[1 + e^{-\epsilon_r(k)/T}\right] + \sum_{q=1}^{\infty} U_{lq} * T\ln\left[1 + e^{-\eta_{r,q}(k)/T}\right] \\
& - \sum_{q=1}^{\infty} S_{lq} * T\ln\left[1 + e^{-\eta_{r-1,q}(k)/T}\right] - \sum_{q=1}^{\infty} S_{lq} * T\ln\left[1 + e^{-\eta_{r+1,q}(k)/T}\right],
\end{aligned}
\tag{A3}
$$

with

$$
U_{lj}(x) = \begin{cases} a_{|l-j|}(x) + 2a_{|l-j|+2}(x) + \ldots + 2a_{l+j-2}(x) + a_{l+j}(x), & l \neq j \\ 2a_2(x) + 2a_4(x) + \ldots + 2a_{2l-2}(x) + a_{2l}(x), & l = j, \end{cases}
$$

$$
S_{lj}(x) = \begin{cases} a_{|l-j|+1}(x) + 2a_{|l-j|+3}(x) + \ldots + 2a_{l+j-3}(x) + a_{l+j-1}(x), & l \neq j \\ a_1(x) + a_3(x) + \ldots + a_{2l-3}(x) + a_{2l-1}(x), & l = j, \end{cases}
$$

while $*$ denotes the convolution $(a * b)(x) = \int a(x - y)b(y)dy$ and the $\eta_{r,l}(k)$ represent the spin string parameters; furthermore $a_n(x) = n|c|/2\pi[(nc/2)^2 + x^2]$. Here

$c = mg_{1D}/\hbar^2 = -2/a_{1D}$. The numerical results used in the figures were obtained by solving the above TBA equations.

Appendix B: Additivity rules for SU(w) Fermi gases

From (4), we find that constant fields in the grand canonical ensemble, i.e. $dH_1 = dH_2 = \ldots = dH_{w-1} = 0$, imply $d\mu_r = d\mu$ for $r = 1, \ldots, w$. Consequently, we have

$$\kappa = \frac{\partial n}{\partial \mu} = \frac{\partial \sum_{r=1}^{w} r n_r}{\partial \mu} = \sum_{r=1}^{w} \frac{r \partial n_r}{\partial \mu_r} = \sum_{r=1}^{w} \kappa_r, \quad \text{(B1)}$$

with κ_r as given by (5) and (6). Note that this result is general and does not use special properties of the SU(w) gases.

The additivity rules for the spin susceptibility are very intriguing. For our convenience in analysis of the SU(w) case, we prefer to keep the ratios among the densities of the charged bound states as $n_1 : n_2 : \ldots : n_{w-1} = \lambda_1 : \lambda_2 : \ldots : \lambda_{w-1}$, then we can parameterize the $n_1, n_2, \ldots, n_w$ as

$$n_r = \frac{\lambda_r}{\lambda} \hat{n}, (r = 1, 2, \ldots, w - 1), \ n_w = \frac{1}{w}(n - \hat{n}) \ \text{(B2)}$$

where $\lambda = \lambda_1 + 2\lambda_2 + \ldots + (w - 1)\lambda_{w-1}$. In order to compute the additivity rules for $\chi_r^{-1} = \partial H_r/\partial M$, with magnetization $M = \sum_{r=1}^{w-1} r(w - r)n_r/2$, we start with the Legendre transformation from Gibbs free energy to ground state energy: $E = G + \mu n + \sum_{r=1}^{w-1} n_r H_r$, and in the ensemble $\{n_1, \cdots, n_{w-1}, n\}$ the field H_r can be obtained:

$$H_r = \frac{\partial E}{\partial n_r}\Big|_{n_1, \cdots, n_{r-1}, n_{r+1}, \cdots, n_{w-1}, n}$$
$$= \frac{\partial E}{\partial n_r}\Big|_{n_1, \cdots, n_{r-1}, n_{r+1}, \cdots, n_w} - \frac{r}{w} \frac{\partial E}{\partial n_r}\Big|_{n_1, \cdots, n_{w-1}} \quad \text{(B3)}$$

where $E = \sum_{r=1}^{w} E_r$ denotes the energy of the multi-component ground state [27] and we have $\partial E/\partial n_r = r\mu_r$ for consistency with (4). We emphasize that the additivity of E is a fundamental property of a TLL, implied by the linearity of the dispersions [27].

Following the relation (B2), we can define differential forms of any thermodynamic function $f = f(n_1, \cdots, n_w)$:

$$\mathrm{d}\,f = \sum_{r=1}^{w-1} \frac{\partial f}{\partial n_r} \cdot \frac{\lambda_r}{\lambda} \Delta \hat{n} - \frac{\partial f}{\partial n_w} \frac{1}{w} \Delta \hat{n}, \quad \text{(B4)}$$

$$\mathrm{d}\,M = \sum_{r=1}^{w-1} \frac{1}{2} r(w - r) \frac{\lambda_r}{\lambda} \cdot \Delta \hat{n}. \quad \text{(B5)}$$

We denote the operator $\mathcal{D}_r = \frac{\partial}{\partial n_r} - \frac{r}{w} \cdot \frac{\partial}{\partial n_w}$ with $r = 1, 2, \ldots, w - 1$. Then the field H_r can be expressed

explicitly: $H_r = \mathcal{D}_r E$ and the susceptibility in response to the H_r can be expressed as

$$\frac{1}{\chi_r} = \frac{\mathrm{d}\,H_r}{\mathrm{d}\,M} = \frac{\sum_{r=1}^{w-1} \lambda_r \mathcal{D}_r}{\sum_{r=1}^{w-1} \frac{1}{2} r(w - r)\lambda_r} \cdot \mathcal{D}_r E.$$

We note that the last term in the Eq. (B3) linearly depends on the density n_r and n_w. Therefore it can be safely dropped off in the calculation of the susceptibilities because of the second order of derivatives. In terms of the ground state energies $E = \sum_{\ell=1}^{w} E_\ell$ for the individual charge bound states We define the stiffness as

$$\frac{1}{\chi_{r\ell}} = \frac{\hbar\pi}{r^2} D_{r,l}^{\chi} = \frac{\sum_{r=1}^{w-1} \lambda_r \mathcal{D}_r}{\sum_{r=1}^{w-1} \frac{1}{2} r(w - r)\lambda_r} \cdot \mathcal{D}_r E_\ell, \quad \text{(B6)}$$

where $r = 1, 2, \ldots, w - 1$ and $\ell = 1, 2, \ldots, w$. Consequently, we have the susceptibility (10) in responses to the external field H_r.

In fact, Zeeman splitting can be characterized by the Zeeman energy levels ϵ_Z^r or by the effective magnetic fields H_r with $r = 1, 2, \ldots, w$. Here $H_w = 0$. Both sets of parameters are related via the relation

$$\sum_{r=1}^{w} \epsilon_Z^r n^r = -\sum_{r=1}^{w} H_r(n^r - n^{r+1}). \quad \text{(B7)}$$

A consistent solution of this equation gives the relations between H_r and Zeeman energy levels [45]. If we denote the difference between the energy levels of fermions in the states $|m + 1\rangle$ and $|m\rangle$ as $\Delta_{m+1,m} = \epsilon_Z^{m+1} - \epsilon_Z^m$, then the total susceptibility $\chi = \frac{\mathrm{d}\,M}{\mathrm{d}\,\Delta_{\text{total}}}$ with $\Delta_{\text{total}} = \sum_{r=1}^{w-1} \Delta_{r+1,r}$ is given by

$$\chi^{-1} = \frac{\mathrm{d}\sum_{r=1}^{w-1} \Delta_{r+1,r}}{\mathrm{d}\,M} = \frac{\mathrm{d}\,(H_1 + H_{w-1})}{\mathrm{d}\,M}$$
$$= \frac{1}{\chi_1} + \frac{1}{\chi_{w-1}}. \quad \text{(B8)}$$

Using the numerical calculation for the Gibbs free energy $G(\mu, H_1, H_2)$ from Eq. (A1), we observe that the susceptibilities χ_1 and χ_2 satisfy the relation (10) in the TLL phase of trions, pairs and single atoms, see Fig. A1.

Using the TBA equations [28, 45], one can easily prove that the specific heat can be written in terms of sound velocities, i.e.

$$c_V = \frac{\pi^2 k_B^2 T}{3} \sum_{r}^{w} \frac{1}{\hbar\pi v_r}. \quad \text{(B9)}$$

Appendix C: Scaling forms on boundaries

We focues on the low temperature behaviour for $w = 3$ to derive the analytical results for the thermodynamics, and finally we derive formula of general SU(w) gases of
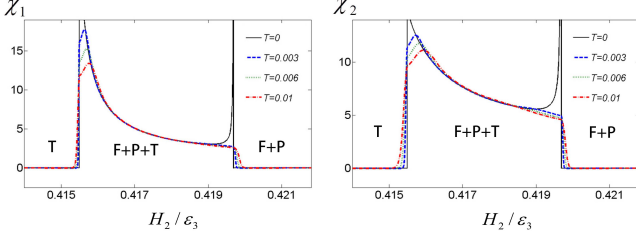
FIG. A1: Susceptibilities in response to H_1 and H_2 for the three-component Fermi gas with a fixed ratio of $n_1/n_2 = 1$ at finite temperatures. Under this setting the H_1 and H_2 have a one-to-one mapping along the line of $n_1/n_2 = 1$ with a fixed total density. These two figures show that the susceptibility is temperature-independent for the TLL phase of F+P+T indicated by the long dashed line in Fig. 3 in the main text. The deviation from the solid lines in the two figures show a breakdown of the TLL. Here T, B and F stand for trions, pairs and excess fermions, respectively. The solid lines confirm the additivity rule Eq. (10) in the main text.

the cricarity about susceptibilities. In the strong interaction limit, we can solve these TBA equations analytically at low temperatures $T \ll \epsilon_3/k_B$ by simplifying

$$\varepsilon_r(k) \approx r\,k^2 - A_r, \qquad r = 1, 2, 3, \qquad \text{(C1)}$$

with

$$
\begin{aligned}
A_1 &= \mu + H_1 - \frac{2}{|c|}p_2 - \frac{2}{3|c|}p_3 + \frac{1}{4|c|^3}Y_{2,\frac{5}{2}} \\
&\quad + \frac{1}{9|c|^3}Y_{3,\frac{5}{2}} + Te^{-(2H_1-H_2)/T}e^{-J_1/T}I_0(J_1/T) \\
A_2 &= 2\mu + \frac{1}{2}c^2 + H_2 - \frac{4}{|c|}p_1 - \frac{1}{|c|}p_2 - \frac{16}{9|c|}p_3 \\
&\quad + \frac{8}{|c|^3}Y_{1,\frac{5}{2}} + \frac{1}{4|c|^3}Y_{2,\frac{5}{2}} + \frac{224}{243|c|^3}Y_{3,\frac{5}{2}} \\
&\quad + Te^{-(2H_2-H_1)/T}e^{-J_2/T}I_0(J_2/T), \\
A_3 &= 3\mu + 2c^2 - \frac{2}{|c|}p_1 - \frac{8}{3|c|}p_2 - \frac{1}{|c|}p_3 \\
&\quad + \frac{1}{2|c|^3}Y_{1,\frac{5}{2}} + \frac{28}{27|c|^3}Y_{2,\frac{5}{2}} + \frac{1}{16|c|^3}Y_{3,\frac{5}{2}} \qquad \text{(C2)}
\end{aligned}
$$

with $Y_{r,a} = -\sqrt{\frac{r}{4\pi}}T^a \text{Li}_a\left(-e^{A_r/T}\right)$. Here the effective spin coupling constant is $J_r = 2p_r/r|c|$ with $c = mg_{1D}/\hbar^2$. The polylogarithm function is defined as $\text{Li}_n(x) = \sum_{k=1}^{\infty}\frac{x^k}{k^n}$ and $I_0(x) = \sum_{k=0}^{\infty}\frac{1}{(k!)^2}\left(x/2\right)^{2k}$. The effective pressures p_r, with $r = 1, 2, 3$, of excess fermions, pairs and trions, respectively, can be expressed as

$$
\begin{aligned}
p_1 &= Y_{1,\frac{3}{2}}\left[1 + \frac{4}{|c|^3}Y_{2,\frac{3}{2}} + \frac{1}{3|c|^3}Y_{3,\frac{3}{2}}\right], \\
p_2 &= Y_{2,\frac{3}{2}}\left[1 + \frac{4}{|c|^3}Y_{1,\frac{3}{2}} + \frac{1}{4|c|^3}Y_{2,\frac{3}{2}} + \frac{112}{81|c|^3}Y_{3,\frac{3}{2}}\right], \\
p_3 &= Y_{2,\frac{3}{2}}\left[1 + \frac{1}{3|c|^3}Y_{1,\frac{3}{2}} + \frac{112}{81|c|^3}Y_{2,\frac{3}{2}} + \frac{1}{8|c|^3}Y_{3,\frac{3}{2}}\right].
\end{aligned}
$$

1. Vacuum – Pair

The above simplified TBA equations (C1) can be used to derive universal low temper properties of the SU(2) and SU(3) Fermi gases. In the following, we derive the scaling forms of the Wilson ratios in the critical regions for the two-component Fermi gas. Here we will use the dimensionless units as being explained in the main text. The phase boundary for the phase transition from V to P phase are $\tilde{\mu}_c = -\frac{1}{2}$ for $h = H/\varepsilon_2 < 1$. Near this critical point, the scaling forms of specific heat, compressibility and susceptibility in dimensionless units are given by

$$\frac{c_V}{|c|t} \approx -\frac{2}{\sqrt{\pi t}}\mathcal{G}\left(\frac{2(\tilde{\mu} - \tilde{\mu}_c)}{t}\right), \qquad \text{(C3)}$$

$$\tilde{\kappa} \approx -\frac{2}{\sqrt{\pi t}}\mathcal{F}\left(\frac{2(\tilde{\mu} - \tilde{\mu}_c)}{t}\right), \qquad \text{(C4)}$$

$$\tilde{\chi} \approx 0. \qquad \text{(C5)}$$

where the functions $\mathcal{G}(x) = \frac{3}{16}\text{Li}_{\frac{3}{2}}(-e^x) - \frac{1}{4}x\text{Li}_{\frac{1}{2}}(-e^x) + \frac{1}{4}x^2\text{Li}_{-\frac{1}{2}}(-e^x)$ and $\mathcal{F}(x) = \text{Li}_{-\frac{1}{2}}(-e^x)$.

2. Vacuum – Fully Polarized

The phase boundary for the phase transition from V to F phase are $\tilde{\mu}_c = -\frac{h}{2}$, for $h > 1$; the scaling forms in dimensionless units are

$$\frac{c_V}{|c|t} \approx -\frac{1}{2\sqrt{2\pi t}}\mathcal{H}\left(\frac{\tilde{\mu} - \tilde{\mu}_c}{t}\right), \qquad \text{(C6)}$$

$$\tilde{\kappa} \approx -\frac{1}{2\sqrt{2\pi t}}\mathcal{F}\left(\frac{\tilde{\mu} - \tilde{\mu}_c}{t}\right), \qquad \text{(C7)}$$

$$\tilde{\chi} \approx -\frac{1}{8\sqrt{2\pi t}}\mathcal{F}\left(\frac{\tilde{\mu} - \tilde{\mu}_c}{t}\right), \qquad \text{(C8)}$$

where $\mathcal{H}(x) = \frac{3}{4}\text{Li}_{\frac{3}{2}}(-e^x) - x\text{Li}_{\frac{1}{2}}(-e^x) + x^2\text{Li}_{-\frac{1}{2}}(-e^x)$.

3. Pair – Partially Polarized

The critical fields for the phase transition from P to F+P phase are $\tilde{\mu}_c = -\frac{h}{2} + \frac{4}{3\pi}(1 - h)^{\frac{3}{2}}$, for $h < 1$; the scaling forms are

$$\frac{c_V}{|c|t} \approx -\frac{1}{2\sqrt{2\pi t}}\mathcal{R}\left(\frac{\tilde{\mu} - \tilde{\mu}_c}{t}\right), \qquad \text{(C9)}$$

$$\tilde{\kappa} \approx \kappa_{o1} - \frac{\lambda_1}{2\sqrt{2\pi t}}\mathcal{F}\left(\frac{\tilde{\mu} - \tilde{\mu}_c}{t}\right), \qquad \text{(C10)}$$

$$\tilde{\chi} \approx -\frac{\lambda_2}{8\sqrt{2\pi t}}\mathcal{F}\left(\frac{\tilde{\mu} - \tilde{\mu}_c}{t}\right), \qquad \text{(C11)}$$

where $b = (1 - h)\left(1 + \frac{2}{\pi}\sqrt{1 - h}\right)$, $\lambda_1 = 1 + \frac{2\sqrt{b}}{\pi} - \frac{10b}{\pi^2}$, $\lambda_2 = 1 - \frac{3\sqrt{b}}{\pi} + \frac{6b}{\pi^2}$, $\kappa_{o1} = \frac{2}{\pi\sqrt{b}}\lambda_1$ and $\mathcal{R}(x) = \frac{3}{4}\text{Li}_{\frac{3}{2}}(-e^x) - x\text{Li}_{\frac{1}{2}}(-e^x) + x^2\text{Li}_{-\frac{1}{2}}(-e^x)$.

4. Fully – Partially Polarized

For the phase transition from F to F+P phase, we have $\tilde{\mu}_c = -\frac{1}{2} + \frac{1}{3\pi}(h-1)^{\frac{3}{2}}$, $h > 1$; with scaling forms

$$\frac{c_V}{|c|t} \approx -\frac{1}{2\sqrt{2\pi t}}\mathcal{S}\left(\frac{2(\tilde{\mu} - \tilde{\mu}_c)}{t}\right), \tag{C12}$$

$$\tilde{\kappa} \approx \kappa_{o3} - \frac{\lambda_3}{2\sqrt{2\pi t}}\mathcal{F}\left(\frac{2(\tilde{\mu} - \tilde{\mu}_c)}{t}\right), \tag{C13}$$

$$\tilde{\chi} \approx \chi_{o4} - \frac{\lambda_4}{8\sqrt{2\pi t}}\mathcal{F}\left(\frac{2(\tilde{\mu} - \tilde{\mu}_c)}{t}\right). \tag{C14}$$

where the constants are given by $a = (h - 1)\left(1 + \frac{2}{3\pi}\sqrt{h-1}\right)$, $\lambda_3 = 4\sqrt{2}\left(1 + \frac{\sqrt{a}}{\sqrt{2\pi}} - \frac{a}{\pi^2}\right)$, $\lambda_4 = \frac{8\sqrt{2}a}{\pi^2}$, $\kappa_{o3} = \frac{1}{2\sqrt{2\pi}\sqrt{a}}$, and $\chi_{o4} = \frac{1}{8\sqrt{2\pi}\sqrt{a}}\left(1 - \frac{3\sqrt{a}}{\pi}\right)$. The dimensionless function is given by $S(x) = \frac{3}{2\sqrt{2}}\mathrm{Li}_{\frac{3}{2}}(-e^x) - \sqrt{2}x\mathrm{Li}_{\frac{1}{2}}(-e^x) + \sqrt{2}x^2\mathrm{Li}_{-\frac{1}{2}}(-e^x)$. The slopes of the Wilson ratio curves at the critical point $\mu = \mu_c$ reveal a unique temperature-dependent feature, namely the slope at the critical point, $\left(\frac{\partial R_w^\kappa}{\partial \mu}\right)_{\mu_c} \equiv \frac{C_r}{T}$ is given as

$$c_r = \frac{r\pi^2}{3}\frac{(\mathcal{F}'(0)\mathcal{G}(0) - \mathcal{F}(0)\mathcal{G}'(0))}{\mathcal{G}(0)^2}, \tag{C15}$$

i.e. is a constant for the phase transition from vacuum into an r-complex TLL phase.

5. Susceptibilities for the gaped phase in the attractive $SU(w)$ gases

The total polarization of $SU(w)$ gas can be expressed as $\tilde{m} = \sum_{r=1}^{w}\frac{1}{2}\tilde{n}_r r(w-r)$, then we can obtain the susceptibility:

$$\tilde{\chi}_r = \frac{\partial \tilde{m}}{\partial \tilde{h}_r} = \sum_{k,l=1}^{w}\frac{1}{2}k(w-k)\frac{\partial^2 \tilde{p}^{(l)}}{\partial \tilde{h}_k \partial \tilde{h}_r} \tag{C16}$$

in the limit of $t \to 0$ and $|c| >> 1$, the leading behavior of the second order derivatives of pressures reads

$$\frac{\partial^2 \tilde{p}^l}{\partial \tilde{h}_k \partial \tilde{h}_r} \approx -\frac{\sqrt{r}}{2}\frac{t^{-\frac{1}{2}}}{\sqrt{\pi}}\mathrm{Li}_{-\frac{1}{2}}(-e^{\frac{\tilde{A}^{(r)}}{t}})\delta_{l,k}\delta_{l,r}. \tag{C17}$$

Substituting (C17) into (C16), we arrive at the explicit form of the susceptibility $\tilde{\chi}_r$ corresponding to the field H_r when the other fields are fixed

$$\tilde{\chi}_r \approx -\frac{t^{-\frac{1}{2}}}{4\sqrt{2\pi}}\sqrt{r}(w-r)r\,\mathrm{Li}_{-\frac{1}{2}}(-e^{\frac{\tilde{A}^{(r)}}{t}})$$

$$\approx \frac{t^{-\frac{1}{2}}}{4\sqrt{2\pi}}\sqrt{r}(w-r)r\,e^{-\frac{\Delta_r}{t}}, \tag{C18}$$

where the gap Δ_r is related to the effective chemical potential through $\Delta_r = -\tilde{A}^{(r)}$, which can be determined from the TBA equations

$$\tilde{A}^{(r)} = r\tilde{\mu} - \sum_{m=1}^{w}\sum_{\substack{q=1 \\ 2q \neq r+m}}^{\min(r,m)}\frac{4\tilde{p}^m}{m(r+m-2q)}. \tag{C19}$$

Here the second approximately equal in (C18) holds when $\Delta_r > 0$ which implies the existence of the gap and the susceptibility presents exponential decay, otherwise $\tilde{\chi}_r \approx \frac{\sqrt{r}(w-r)r}{4\sqrt{2\pi}\sqrt{-\Delta_r}}$, which is a positive constant when $t \to 0$. Note that the result in (C18) is different by a factor $\frac{1}{2}$ due to the convention of $H_1 = H/2$ in the SU(2) case.

Appendix D: Explicit formulas for the SU(2) Fermi gas

In the mixed phase for SU(2) Fermi gas with one magnetic field H_1, we have $n = 2n_2 + n_1$ and $\chi_{1,1} = (\mu_B\mathfrak{g})^2\left(\partial n_1/\partial \mu_1\right)_n$, $\chi_{1,2} = 2(\mu_B\mathfrak{g})^2\left(\partial n_2/\partial \mu_2\right)_n$, with the stiffnesses in canonical ensemble $D_1^\chi = \frac{1}{\hbar\pi}\left(\partial \mu_1/\partial n_1\right)_n$, $D_2^\chi = \frac{2}{\hbar\pi}\left(\partial \mu_2/\partial n_2\right)_n$. Similarly, $\kappa_1 = \left(\partial n_1/\partial \mu_1\right)_H$ and $\kappa_2 = 2\left(\partial n_2/\partial \mu_2\right)_H$ with $D_2^\kappa = \frac{2}{\hbar\pi}\left(\partial \mu_2/\partial n_2\right)_H$, $D_1^\kappa = \frac{1}{\hbar\pi}\left(\partial \mu_1/\partial n_1\right)_H$ defined in the grand canonical ensemble.

For strong coupling, we find the explicit form of the μ_r in terms of the densities of pairs n_2 and unpaired fermions n_1 (in units of $\hbar^2/(2m)$) [45] to be

$$\mu_2 \approx \pi^2\left(\frac{n_2^2}{4} + \frac{2n_2^3}{3|c|} + \frac{n_2^2 n_1}{|c|} + \frac{4n_1^3}{3|c|} + \frac{3n_1^2 n_2^2}{c^2} + \frac{5n_2^4}{4c^2}\right.$$

$$\left. + \frac{4n_1 n_2^3}{c^2} + \frac{16n_1^3 n_2}{c^2}\right), \tag{D1}$$

$$\mu_1 \approx \pi^2\left(n_1^2 + \frac{8n_1^2 n_2}{|c|} + \frac{2n_2^3}{3|c|} + \frac{48n_1^2 n_2^2}{c^2} + \frac{4n_2^3 n_1}{c^2}\right.$$

$$\left. + \frac{2n_2^4}{c^2}\right). \tag{D2}$$

Here $c = mg_{1D}/\hbar^2 = -2/a_{1D}$ is the interaction strength. Therefore, the compressibilities and susceptibilities are

given by (in units of $\hbar^2/(2m)$), e.g.

$$
\kappa_2^{-1} \approx \frac{\pi^2 n_2}{4}\left(1 + \frac{6n_1}{|c|} + \frac{4n_2}{|c|} + \frac{n_2^2}{2|c|n_1} + \frac{24n_1^2}{c^2}\right.
$$
$$
\left. + \frac{24n_1 n_2}{c^2} + \frac{17n_2^2}{c^2} - \frac{2n_2^3}{c^2 n_1} + \frac{n_2^4}{4c^2 n_1^2}\right), \quad \text{(D3)}
$$

$$
\kappa_1^{-1} \approx 2\pi^2 n_1\left(1 + \frac{12n_2}{|c|} + \frac{16n_1^2}{|c|n_2} + \frac{96n_2^2}{c^2} + \frac{384n_1^2}{c^2}\right.
$$
$$
\left. - \frac{8n_1 n_2}{c^2} - \frac{96n_1^3}{c^2 n_2} + \frac{256n_1^4}{c^2 n_2}\right) \quad \text{(D4)}
$$

$$
\chi_{1,1}^{-1} = \pi^2 n_2\left[1 + \frac{4}{|c|}(n - 3n_2) + \frac{3}{c^2}(4n^2\right.
$$
$$
\left. - 24nn_2 + 30n_2^2)\right], \quad \text{(D5)}
$$

$$
\chi_{1,2}^{-1} = 8\pi^2 n_1\left[1 + \frac{4}{|c|}(n - 2n_1) + \frac{4}{c^2}(2n^2\right.
$$
$$
\left. + 10n_1^2 - 12nn_1)\right]. \quad \text{(D6)}
$$

In the above calculation for compressibility, the condition $H = 2(\mu_1 - \mu_2) + c^2/4$ was used, i.e. $dH = 0$ gives (up to the $O\left(\frac{1}{c^2}\right)$ order):

$$
\frac{dn_1}{dn_2} = \frac{n_2}{4n_1}\left(1 - \frac{8n_2}{|c|} + \frac{6n_1}{|c|} + \frac{n_2^2}{2|c|n_1} - \frac{16n_1^2}{|c|n_2}\right). \quad \text{(D7)}
$$

Moreover, the interaction effect enters into the collective velocities v_1, v_2 of the excess fermions and bound pairs. For strong attraction, they are given by [27]

$$
v_1 \approx \frac{\hbar}{2m}2\pi n_1\left(1 + 8n_2/|c| + 48n_2^2/c^2\right),
$$
$$
v_2 \approx \frac{\hbar}{2m}\pi n_2\left(1 + 2A/|c| + 3A^2/c^2\right), \quad \text{(D8)}
$$

with $A = 2n_1 + n_2$.

Appendix E: Connection between the Luttinger and Fermi liquids

Wilson Ratios. Now we further build up a connection between the TLL and the Fermi liquid. By definition (1) and (2), the two type of Wilson ratios of interacting Fermi liquid in 3D are given by

$$
R_W^\chi = \frac{1}{1 + F_0^a}, \quad R_W^\kappa = \frac{1}{1 + F_0^s} \quad \text{(E1)}
$$

which depends on Landau parameters $F_0^{a,s}$ charactering the interaction [3]. This is very similar to our finding for 1D systems, see Eqs. (12) and (13). However, it's extremely hard to calculate the Landau parameters $F_{0,1}^{s,a}$ in Fermi liquid theory due to the reason that $N^*(0)$ can not be obtained explicitly. Fermi liquid theory elegantly maps an interacting system into a free fermion system where the interaction is encoded into the density of state and effective mass. But the Fermi liquid theory is not valid in 1D interacting systems because there does not exist a well-defined quasiparticle. Here we demonstrate that exact solution of the TBA equations does show a novel existence of Fermi liquid like signature in 1D interacting systems. In fact, the additivity rules which we found in previous sections reflect a 1D Fermi liquid like nature, also see a discussion in [16].

Feedback interaction. The excitations near Fermi points in 1D many-body systems can form a collective motion independent of microscopic details of systems, namely, there exists a certain dispersion relation between energy and momentum. We observe that integrable systems provide a deep understanding of the intrinsic connection between the TLL and the Fermi liquid. In fact, the TBA equations of 1D systems give the exact dressed energies and determine the dispersion relations of each branch. At low temperatures, only the behavior of the dressed energies near the zero point, or saying, the k_F and v_F at the 1D Fermi points, determines the first order and second orders of thermodynamic quantities. In general, for the attractive $SU(N)$ Fermi gases, the spin fluctuations are suppressed. Therefore the TBA equations can be rewritten as

$$
\varepsilon^{(r)}(k) = \epsilon_r^0(k) - \sum_{s=1}^N A_{rs} * \varepsilon_-^{(s)}(k), \quad (r = 1, 2, \cdots, w),
$$
$$
A_{mn} = \sum_{q=1}^{min(m,n)} a_{m+n-q} \quad \text{(E2)}
$$

where $\epsilon_r^0 = \frac{\hbar^2}{2m}r(k^2 - \mu_r) = \frac{p_0^2}{2rm} - \frac{\hbar^2}{2m}r\mu_r$ is the first order coefficient describing excitation energy of a single r-complex, here μ_r the effective chemical potential. Here $p_0 = r\hbar k$. The function $a_m(x)$ is defined in Appendix A. These equations show a similar form of 'feedback interaction' equation in the Landau Fermi liquid theory [15, 16]. This encourage us to further find a perturbation idea into our calculations. What below gives a Fermi liquid like description for the low energies of the 1D attractive Fermi gases, i.e. mapping an interacting system with multi-subsystems to a multicomponent free system.

Phenomenological description. The symmetry group of the interaction of quasi particles in the 1D "Fermi liquid" is reduced from the $SO(3)$ group to the cyclic group C_2. Therefore, interaction parameter between the 'quasi' momentum p and p' could be written as $f_{p,p'}^{s,a} = f_0^{s,a} + f_1^{s,a}sign(p \cdot p\prime)$. Then following the conventional Fermi liquid theory, we still can have Landau parameters $F_{0,1}^{s,a}$, which are interacting parameters [16] and describe the main properties of our system. Conventional sound velocity is associated with oscillations in the density of a fluid, and hydrodynamics gives that

$$
v^2 = \frac{\kappa}{\rho} = \frac{\kappa}{mn}. \quad \text{(E3)}
$$

Where $\rho = mn$ is the density of the fluid and $\kappa = -L\frac{\partial P}{\partial L}$ is the bulk modulus. In FL theory $\kappa = \frac{n^2}{N^*(0)}(1 + F_0^s)$,

where the $N^*(0)$ denotes the density of state in momentum space near Fermi surface, therefore the velocity of first sound is given by

$$v^2 = \frac{n}{mN^*(0)}(1 + F_0^s) \qquad \text{(E4)}$$

By the 1D analog of Fermi liquid theory, we have the relations [16] $n = \frac{p_F}{\pi}$, $N^*(0) = \frac{1}{\pi}\frac{m^*}{p_F}$ and $m = m^*(1 + F_1^s)$. Then we obtain:

$$v^2 = v_F^2(1 + F_0^s)(1 + F_1^s). \qquad \text{(E5)}$$

Here, due to the collective motion, the backflow does not exist in 1D, therefore $F_1^s \approx 0$. This can be seen from the dressed energy equation (E2), where the effective mass $r\,m$ is almost unchanged up to the order of $O(c^{-2})$ for a strong coupling regime.

Consistency. Using the exact solutions, we can calculate the Wilson ratio R_W^c for different phases of TLLs. For a single state of a r-complex, the Wilson ratio is known from Eq. (E1). Then the parameter $F_{0,1}^s$ could be determined by a comparison with the Bethe ansatz result in strong coupling limit (i.e. $|c| \to \infty$) via

$$R_{\mathrm{W}}^c = \frac{1}{(1 + F_0^s)} = \begin{cases} 1; & \text{for free fermions} \\ 4; & \text{for pairs} \\ 9; & \text{for trions} \end{cases} \qquad \text{(E6)}$$

From the equation (E5) and (E6) we could calculate the relation between Fermi speed and sound velocity. For example, the velocities of trions, pairs and single fermionic atoms, are given by

$$v^3 = \frac{1}{3}v_F^{(3)}; \ \ v^2 = \frac{1}{2}v_F^{(2)}; \ \ v^1 = v_F^{(1)}, \qquad \text{(E7)}$$

respectively. This builds up an intrinsic connection between the Luttinger liquid and Fermi liquid.

Furthermore, from the free fermion nature of the Fermi liquid, we can express the specific heat in terms of these sound velocities

$$\frac{c_V}{T} = \frac{\pi}{3}\left(\frac{1}{v_F^1} + \frac{2}{v_F^2} + \frac{3}{v_F^3}\right) = \frac{\pi}{3}\left(\frac{1}{v^1} + \frac{1}{v^2} + \frac{1}{v^3}\right), \text{(E8)}$$

where we have dropped the unit $k_B^2\hbar^{-1}$, here the interaction effect is encoded in the velocities $v^{1,2,3}$. This equation could be obtained by consiering the leading term of the TBA equations at low temperature region. This shows a consistency of our derivation by the 1D Fermi liquid like description. The derivation above could be extended to the SU(w) attractive Fermi gases in a straightforward way. All the derivation above could be directly extended to the SU(w) attractive Fermi gases:

$$\frac{c_V}{T} = \frac{\pi}{3}\left(\frac{1}{v^1} + \frac{1}{v^2} + \cdots + \frac{1}{v^w}\right). \qquad \text{(E9)}$$

We can also prove this additivity rule using the TBA equations, see Appendix B.

---

[1] Sachdev, S. *Quantum Phase transitions* (Cambridge University Press, Cambridge, 1999).

[2] Pethick, C. J., and H. Smith, 2008, *Bose-Einstein Condensation in Dilute Gases* (Cambridge University Press, Cambridge, England).

[3] A. C. Hewson, *The Kondo Problem to Heavy Fermions* (Cambridge University Press, Cambridge, 1997).

[4] T. Giamarchi, *Quantum Physics in one dimension* (Oxford University Press, Oxford, 2004).

[5] F. H. L. Essler, *et.al. The One-Dimensional Hubbard Model* (Cambridge University Press, Cambridge, 2005).

[6] Cazalilla, M. A., Citro, R., Giamarchi, T., Orignac, E. & Rigol, M. One dimensional bosons: From condensed matter systems to ultracold gases. *Rev. Mod. Phys.* **83**, 1405 (2011).

[7] Imambekov, A., Schmidt, T. L., & Glazman, L. I. One-dimensional quantum liquids: Beyond the Luttinger liquid paradigm. *Rev. Mod. Phys.* 84, 1253 (2012).

[8] Wiedemann, G. and Franz, R. Ueber die Wärme-Leitungsfähigkeit der Metalle *Ann. Phys.* **89**, 497 (1853).

[9] Kadowaki, K. & Woods, S. B. Universal relationship of the resistivity and specific heat in heavy-Fermion compounds *Solid Stat. Commun.* **58**, 507 (1986).

[10] Jacko, A. C., Fjaerestad, J. O. & Powell, B. J. A unified explanation of the Kadowaki-Woods ratio in strongly correlated metals. *Nat. Phys.* **5**, 422 (2009).

[11] Tanatar, M. A., Paglione, J., Petrovic, C., & Taillefer, L. Anisotropic violation of the Wiedemann-Franz law at a quantum critical point. *Science* **316**, 1320 (2007).

[12] Taupin, M. *et al.* Thermal conductivity through the quantum critical point in $YbRh_2Si_2$ at very low temperature. *Phys. Rev. Lett.* **115**, 046402 (2015).

[13] Sommerfeld, A. Zur Elektronentheorie der Metalle auf Grund der Fermischen Statistik (Electron theory on the basis of the Fermi statistics). *Z. Phys.* **47**, 1-32 (1928).

[14] Wilson, K. G. The renormalization group: Critical phenomena and the Kondo problem *Rev. Mod. Phys.* **47**, 773 (1975).

[15] Schofield, A. J. Non-Fermi liquids. *Contemporary Physics* **40**, 95-115 (1999).

[16] Wang, Y. -P. Fermi liquid features of the one-dimensional Luttinger liquid, Int. J. Mod. Phys. B **12**, 3465 (1998).

[17] Ninios, K. *et al.* Wilson ratio of a Tomonaga-Luttinger liquid in a spin-1/2 Heisenberg ladder. *Phys. Rev. Lett.* **108**, 097201 (2012).

[18] Guan, X. -W., Yin, X. -G., Foerster, A., Batchelor, M. T., Lee, C. -H., & Lin, H. Q. Wilson ratio of Fermi gases in one dimension *Phys. Rev. Lett.* **111**, 130401 (2013).

[19] B. Yang, Y.-Y. Chen, Y.-G. Zheng, H. Sun, H.-N. Dai, X.-W. Guan, Y.-Z. Yuan and J.-W. Pan, *Quantum criticality and Luttinger liquid in one-dimensional Bose*

gases, preprint 2016.

[20] Ho, T. L. & Yip, S. Pairing of fermions with arbitrary spin. *Phys. Rev. Lett.* **82**, 247 (1999).

[21] Wu, C., Hu, J. -P. & Zhang, S. -C. Exact SO(5) symmetry in the spin-3/2 fermionic system. *Phys. Rev. Lett.* **91**, 186402 (2003).

[22] Cazalilla, M. A. & Rey, A. M. Ultracold fermi gases with emergent SU(N) symmetry. *Rep. Prog. Phys.* **77** (2014) 124401.

[23] Boettcher, I. *et al.* Equation of state of ultracold fermions in the 2D BEC-BCS crossover. arXiv:1509.03610.

[24] Taie, S. *et al.* An SU(6) Mott insulator of an atomic fermi gas realized by large-spin Pomeranchuk cooling. *Nat. Phys.* **8** 825-830 (2012).

[25] Scazza, F. *et al.* Observation of two-orbital spin-exchange interactions with ultracold SU(N)-symmetric fermions. *Nat. Phys.* **10** 779-784 (2014).

[26] Kono, Y. *et al.* Field-induced quantum criticality and universal temperature dependence of the magnetization of a spin-1/2 Heisenberg chain. *Phys. Rev. Lett.* **114**, 037202 (2015).

[27] Guan, X.-W., Batchelor, M. T. & Lee, C.-H. Fermi gases in one dimension:From Bethe ansatz to experiments. *Rev. Mod. Phys.* **85**, 1633 (2013).

[28] M. Takahashi, *Thermodynamics of One-Dimensional Solvable Models*, (Cambridge University Press, Cambridge, 1999).

[29] Schlottmann, P. Thermodynamics of the one-dimensional multicomponent fermi gas with a delta-fulction interaction. *J. Phys. Condens. Matter* **5**, 5869 (1993).

[30] Guan, X. -W., Batchelor, M. T., Lee, C. & Bortz, M. Phase transitions and pairing signature in strongly attractive Fermi atomic gases. *Phys. Rev. B* **76**, 085120 (2007).

[31] Sutherland, B. Further results for the many-body problem in one dimension. *Phys. Rev. Lett.* **20**, 98 (1968).

[32] Takahashi, M. Ground state energy of the one-dimensional electron system with short-range interaction. *Prog. Theor. Phys.* **44**, 348-358 (1970); Many-body problem of attractive fermions with arbitrary spin in one dimension. **44**, 899-904 (1970).

[33] Olshanii, M. Atomic Scattering in the Presence of an External Confinement and a Gas of Impenetrable Bosons, *Phys. Rev. Lett.* **81**, 938 (1998).

[34] Pagano, G. *et al.* A one-dimensional liquid of fermions with tunable spin *Nat. Phys.* **10**, 198-201 (2014).

[35] Yang, C. -N. Some exact results for the many-body problem in one dimension with repulsive delta-function interaction. *Phys. Rev. Lett.* **19**, 1312 (1967).

[36] Gaudin, M. Un systeme a une dimension de fermions en interaction. *Phys. Lett. A* **24**, 55-56 (1967).

[37] Liao, Y. A.*et. al.* Spin-imbalance in a one-dimensional Fermi gas. *Nature* **467**, 567-569 (2010).

[38] Wenz, A. N.*et. al.* From few to many atoms at a time. *Science* **342**, 457 (2013).

[39] Orso, G. Attractive Fermi gases with unequal spin populations in highly elongated traps. *Phys. Rev. Lett.* **98**, 070402 (2007).

[40] Hu, H., Liu, X. -J. & Drummond, P. D. Phase diagram of a strongly interacting polarized Fermi gas in one dimension. *Phys. Rev. Lett.* **98**, 070403 (2007).

[41] Capponi, S., Roux, G., Lecheminant, P., Azaria, P., Boulat, E. & White, S. R. Molecular superfluid phase in systems of one-dimensional multicomponent fermionic cold atoms, *Phys. Rev. A* **77**, 013624 (2008).

[42] Gegenwart, P., Si, Q. & Steglich F., Quantum criticality in heavy-fermion metals, *Nat. Phys.* **4**, 186 (2008).

[43] Guan, X. -W., Batchelor, M. T., Lee, C. & Zhou, H. -Q. Magnetic phase transitions in one-dimensional strongly attractive three-component ultracold fermions. *Phys. Rev. Lett.* **100**, 200401 (2008).

[44] Kuhn, C. C. N. & Foerster, A. Phase diagrams of three-component attractive ultracold fermions in one dimension. *New J. Phys.* **14**, 013008 (2012).

[45] Lee, J.-Y. Guan, X.-W. and Batchelor, M. T. Yang-Yang method for the thermodynamics of one-dimensional multi-component interacting fermions. *J. Phys. A: Math. Theor.* **44**, 165002 (2011).

[46] Cheng, C. H. & Yip, S. K. Trapped resonant fermions above the superfluid transition temperature. *Phys. Rev. B* **75**, 014526 (2007).

[47] Ho, T. L. & Zhou, Q. Obtaining the phase diagram and thermodynamic quantities of bulk systems from the densities of trapped gases, *Nature Physics*, **6**, 131 (2010).

[48] Andrews, M. R. *et. al.* Propagation of sound in a Bose-Einstein condensate. *Phys. Rev. Lett.* **79**, 553 (1997).

[49] Affleck I. and Haldane F. D. M., *Phys. Rev. B* **36**, 5291 (1987).

[50] Frahm H. and Korepin V. E., Phys. Rev. B **42**, 10553 (1990); Frahm H. and Korepin V. E., Phys. Rev. B **43**, 5653 (1991).